AD/A

ESD-TR-85-323

Technical Report
727

Cramér-Rao Bound Analysis for Frequency Estimation of Sinusoids in Noise

J.M. Skon

24 March 1986

Lincoln Laboratory

MASSACHUSETTS INSTITUTE OF TECHNOLOGY

LEXINGTON, MASSACHUSETTS

Prepared for the Department of the Army
under Electronic Systems Division Contract F19628-85-C-0002.

The work reported in this document was performed at Lincoln Laboratory, a center for research operated by Massachusetts Institute of Technology, with the support of the Department of the Air Force under Contract F19628-85-C-0002.

This technical report has been reviewed and is approved for publication.

FOR THE COMMANDER

Thomas J. Alpert, Major, USAF
Chief, ESD Lincoln Laboratory Project Office

MASSACHUSETTS INSTITUTE OF TECHNOLOGY
LINCOLN LABORATORY

CRAMÉR-RAO BOUND ANALYSIS FOR FREQUENCY ESTIMATION OF SINUSOIDS IN NOISE

J.M. SKON
Group 32

TECHNICAL REPORT 727

24 March 1986

LEXINGTON MASSACHUSETTS

ABSTRACT

The Cramér-Rao inequality is used to determine a lower bound on the variance with which a sinusoidal frequency can be estimated in the presence of Gaussian white noise. A parametric study has elucidated the influence of number of samples (N), sampling frequency ($1/\Delta$), phase (ϕ), and signal-to-noise ratio (SNR) on the Cramér-Rao bound. A closed form expression for the asymptotic level to which the Cramér-Rao bound decays is characterized and, for low frequencies, the bound is determined analytically and graphically. The form of the Cramér-Rao bound is linked to resolution in the sampling problem. Identification of trade-offs characterizing the sensitivity of the bound and parameters associated with it are discussed.

TABLE OF CONTENTS

LIST OF ILLUSTRATIONS

LIST OF TABLES

CRAMÉR-RAO BOUND ANALYSIS FOR FREQUENCY ESTIMATION OF SINUSOIDS IN NOISE

I. INTRODUCTION

A problem of interest is estimation of the frequency of a sinusoidal oscillation from noisy sampled data. The particular emphasis in this report is on the case in which only a fraction of a cycle is sampled. It is hoped that the guidance achieved in solving this problem could be applied to the more complex problem of motion other than a pure sinusoid. The approach here is to use the Cramér-Rao bound as a calculation tool. The Cramér-Rao bound is a lower bound on the variance in parameter estimation in the case when the estimator is unbiased.

The problem of frequency estimation for single and multiple complex sinusoids in noise has received attention in the literature [1, 2] for the case of frequency large compared with the reciprocal of the measurement interval ($1/N\Delta$). A maximum likelihood method for frequency estimation of real sinusoids in noise, with improved computation efficiency, has already been presented [3]. Of interest to the problem of determination of frequencies is the case in which the observation period $N\Delta$ (N = number of samples, Δ = sampling interval) is short compared with the oscillation period. In this case a good signal-to-noise ratio (SNR) can compensate for the short measurement interval.

Examination of the Cramér-Rao bound follows its derivation from the original problem of sampling a sine wave. A frequency independent form for the Cramér-Rao bound is presented which is accurate for frequencies between those designated by the Nyquist criterion. The frequency dependence of the bound at low frequencies, for initial phases of 0 and $\pi/2$, is obtained. Finally, the family of Cramér-Rao bound curves parameterized by N and Δ is reduced to a single operating curve from which trade-offs involving $N\Delta$ and SNR, as well as an expression for the bound for low frequencies, are determined.

II. DERIVATION OF THE CRAMÉR-RAO BOUND

The general problem of estimation of a sinusoidal frequency in Gaussian white noise derives from taking N samples of the system separated by successive sampling intervals Δ

$$Y_i = S_i + W_i \quad , \quad S_i = A \sin(2\pi f \Delta i + \phi) \quad , \quad (i = 1 \ldots N) \tag{1}$$

where A, f, and ϕ are oscillation amplitude, frequency, and phase. The measurement errors W_i are Gaussian and independently distributed with zero mean and variance σ_R^2. Since the $(Y_i - S_i) = W_i$ are therefore also Gaussian, the probability density function for these terms can be represented:

$$p(\vec{Y}/\vec{S}) = \frac{1}{(2\pi)^{N/2}\sigma_R^N} \exp\left[-\frac{1}{2} \sum_{i=1}^{N} (Y_i - S_i)^2/\sigma_R^2\right] \tag{2}$$

The Cramér-Rao inequality is a lower bound on the variance in parameter estimation and is derived from the Fisher information matrix [4, 5]. This matrix can be expressed as follows:

$$E\left[\left(\frac{d \ln P(\vec{Y}/\vec{S})}{d\underline{\alpha}}\right)^2\right] \quad \text{where } \underline{\alpha} = \begin{bmatrix} A \\ f \\ \phi \end{bmatrix} \tag{3}$$

$\ln P(\vec{Y}/\vec{S})$ is the log likelihood function which can be discerned from the above density function as

$$\ln P(\vec{Y}/\vec{S}) = -1/2 \sum_{i=1}^{N} (Y_i - S_i)^2/\sigma_R^2 \tag{4}$$

ignoring the constant terms. The derivative of the log likelihood function with respect to the parameters of the sinusoid,

$$\underline{\alpha} = \begin{bmatrix} A \\ f \\ \phi \end{bmatrix} \quad , \quad \text{is}$$

$$\frac{d \ln P(\vec{Y}/\vec{S})}{d\underline{\alpha}} = \sum_{i=1}^{N} (Y_i - S_i) \frac{dS_i}{d\underline{\alpha}} \frac{1}{\sigma_R^2} \tag{5}$$

Squaring this expression and taking its expectation results in:

$$E\left[\left(\frac{d \ln P(\vec{Y}/\vec{S})}{d\underline{\alpha}}\right)^2\right] = E\left[\sum_{i=1}^{N} \sum_{j=1}^{N} \frac{(Y_i - S_i)(Y_j - S_j)}{\sigma_R^4} \frac{dS_i}{d\alpha} \frac{dS_j^T}{d\alpha}\right] \tag{6}$$

$E[(Y_i - S_i)(Y_j - S_j)] = 0$ except at i = j where it equals σ_R^2.

$$\text{Thus } E\left[\frac{d \ln P(\vec{Y}/\vec{S})}{d\underline{\alpha}}\right]^2 = \sum_{i=1}^{N} \frac{1}{\sigma_R^2} \frac{dS_i}{d\underline{\alpha}} \frac{dS_i^T}{d\underline{\alpha}} , \tag{7}$$

$$\text{where } \frac{dS_i}{d\underline{\alpha}} = \begin{bmatrix} \frac{\partial S_i}{\partial A} \\ \frac{\partial S_i}{\partial f} \\ \frac{\partial S_i}{\partial \phi} \end{bmatrix}$$

and each element (jk) of the resulting Fisher information matrix

$$\text{B equals } \sum_{i=1}^{N} \frac{1}{\sigma_R^2} \frac{\partial S_i}{\partial \alpha_j} \frac{\partial S_i}{\partial \alpha_k} .$$

It is the inverse of B which yields the Cramér-Rao bound on estimation of the α_j. The Cramér-Rao bound can be stated as

$$\text{Var } (\hat{\alpha}^j - \alpha^j) \geq B^{jj}$$

where $\hat{\alpha}_j$ is an unbiased estimate of α_j and B^{jj} is the jth diagonal element of the inverse of B.

The matrix B to be inverted is symmetric and is shown explicitly below:

$$B_{11} = \sum_{i=1}^{N} \frac{1}{\sigma_R^2} (\sin (2\pi f \Delta i + \phi))^2$$

$$B_{22} = \sum_{i=1}^{N} \frac{1}{\sigma_R^2} (2\pi \Delta i A \cos (2\pi f \Delta i + \phi))^2$$

$$B_{33} = \sum_{i=1}^{N} \frac{1}{\sigma_R^2} (A \cos (2\pi f \Delta i + \phi))^2 \tag{8}$$

$$B_{12} = B_{21} = \sum_{i=1}^{N} \frac{1}{\sigma_R^2} (2\pi \Delta i A \sin (2\pi f \Delta i + \phi) \cos (2\pi f \Delta i + \phi))$$

$$B_{13} = B_{31} = \sum_{i=1}^{N} \frac{1}{\sigma_R^2} (A \sin (2\pi f \Delta i + \phi) \cos (2\pi f \Delta i + \phi))$$

$$B_{23} = B_{32} = \sum_{i=1}^{N} \frac{1}{\sigma_R^2} (2\pi \Delta i (A \cos (2\pi f \Delta i + \phi))^2)$$

Rather than working with the Cramér-Rao bound in terms of variance, the root mean square error in frequency estimation, $(B^{22})^{1/2}$, will be used here whenever the Cramér-Rao bound is referred to subsequently. $(B^{11})^{1/2}$ and $(B^{33})^{1/2}$ are the Cramér-Rao bounds for estimation of amplitude and phase, respectively. (A/σ_R) is the square root of the signal-to-noise ratio $(\sqrt{SNR})$ and is taken to be equal to 1 everywhere except in Section VI.

III. NUMERICAL RESULTS: PHASE (ϕ) = 0

One of the first eharaeteristies of the Cramér-Rao bound with whieh to be eoneerned is its behavior at the Nyquist frequeney $1/\Delta = 2f$. This eorresponds to the ease in whieh the sinusoidal frequeney is sampled exaetly at its nodes. Sinee frequeney estimation is then impossible, the Cramér-Rao bound is infinite. For $f = k/2\Delta$ (where $k = 1, 2 \ldots$) the infinity repeats for higher frequeneies. Figure 1 shows the behavior of the Cramér-Rao bound for the sampling parameters $N = 16$, $\Delta = 0.008$. The Cramér-Rao bound $(B^{22})^{1/2}$ is eomputed from (8) and is singular at $f = 1/2\Delta \approx 62.5$ and all multiples.

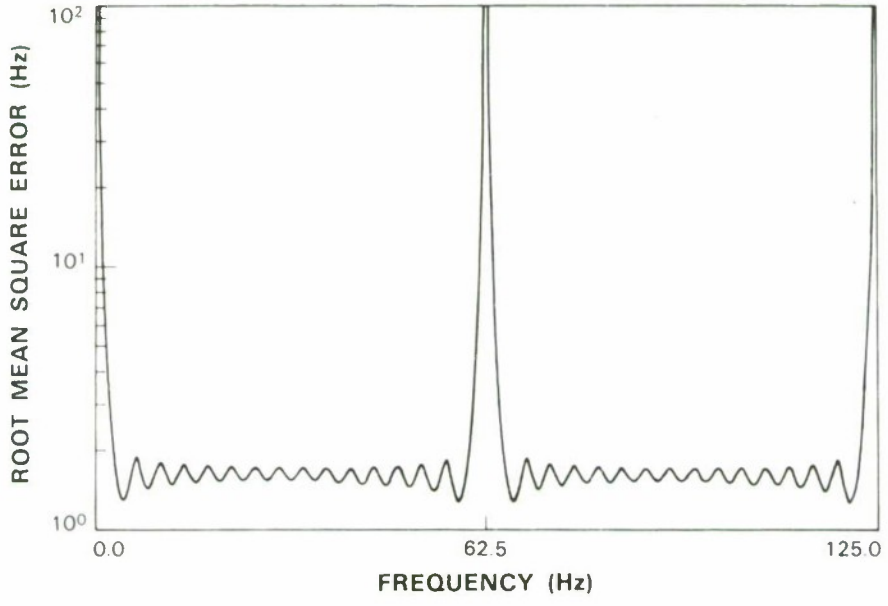

73645-1

Figure 1. Nyquist intervals of Cramér-Rao bound. $N = 16$, $\Delta = 0.008$, $\phi = 0$.

The following figure exhibits the Cramér-Rao bound behavior for frequeneies mueh less than the Nyquist frequeney. The Cramér-Rao bound $(B^{22})^{1/2}$ eomputed from (8) is plotted in Figure 2, taking $N = 16$, 32, 64, 128, 256 and 512 sueeessive samples separated in time by a eonstant interval of $\Delta = 0.008$ s. It is immediately obvious that the Cramér-Rao bound deereases when N, the number of samples taken, inereases. The break point between the monotonie and oseillatory parts of eaeh eurve oeeurs at $f = 1/2N\Delta$ whieh is at inereasingly lower frequeney as N beeomes greater. The third trend is that the Cramér-Rao bound deeays to an asymptotie level as frequency inereases. $\sqrt{SNR}$ has been taken to be 1 here, however, it is implieit from Equations (8) for B^{22} that the Cramér-Rao bound shown in Figures 1 and 2 should be divided by $\sqrt{SNR}$ in the more general ease.

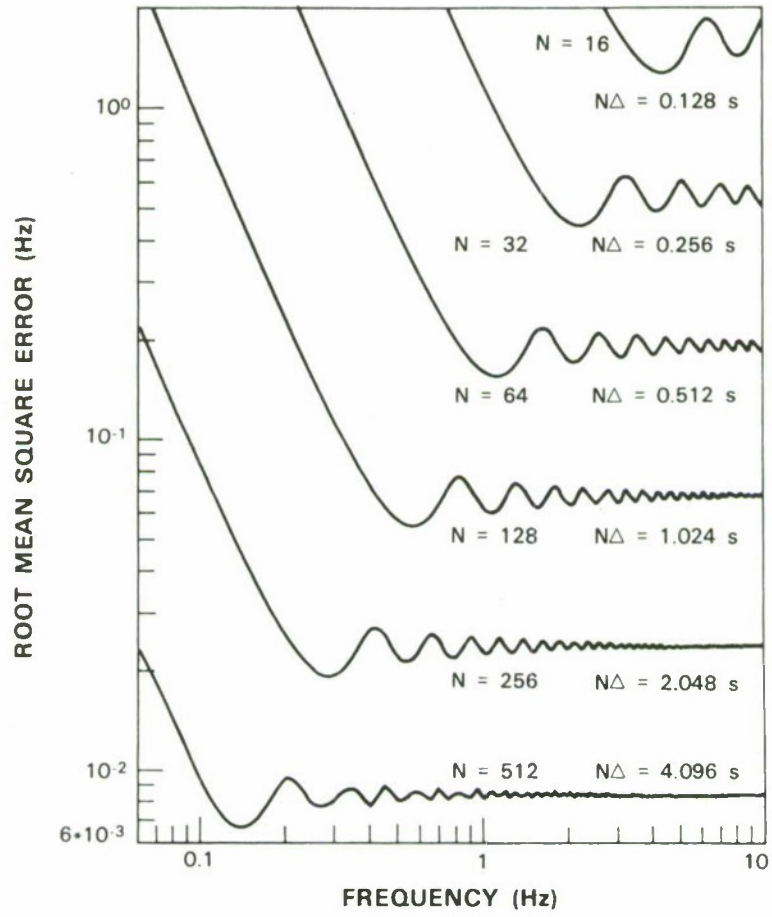

73645-2

Figure 2. Cramér-Rao bound for frequency estimation. Δ = 0.008, ϕ = 0.

Figure 3 exhibits the Cramér-Rao bound for $N\Delta = 1$. The family of curves consists of the cases in which N = 16, 32, 64, 128, 256 and 512 are matched with Δ = 0.0625, 0.0313, 0.0156, 0.0078, 0.0039, and 0.002 respectively. The break point is now at approximately $f = 1/2N\Delta \approx 0.5$ Hz for all six curves. For the portions of curves shown in Figure 3, the oscillatory parts of the bounds are identical except for an offset in asymptotic level.

On account of the Nyquist criterion, for which sampling is only at nodes of a sinusoid, infinities repeat for $f = 1/2\Delta \approx (k = 1, 2 \ldots)$. For the case in Figure 2 these infinities repeated at the same frequency for all curves. Each of the curves in Figure 3, however, has its own period imposed by the Nyquist criterion as Δ is different for each. Thus the N = 16 curve in Figure 3 will give rise to a singularity at $f \approx 8$, the N = 32 curve at $f \approx 16$, and so on. Our primary interest, however, is in the low frequency portions of these curves.

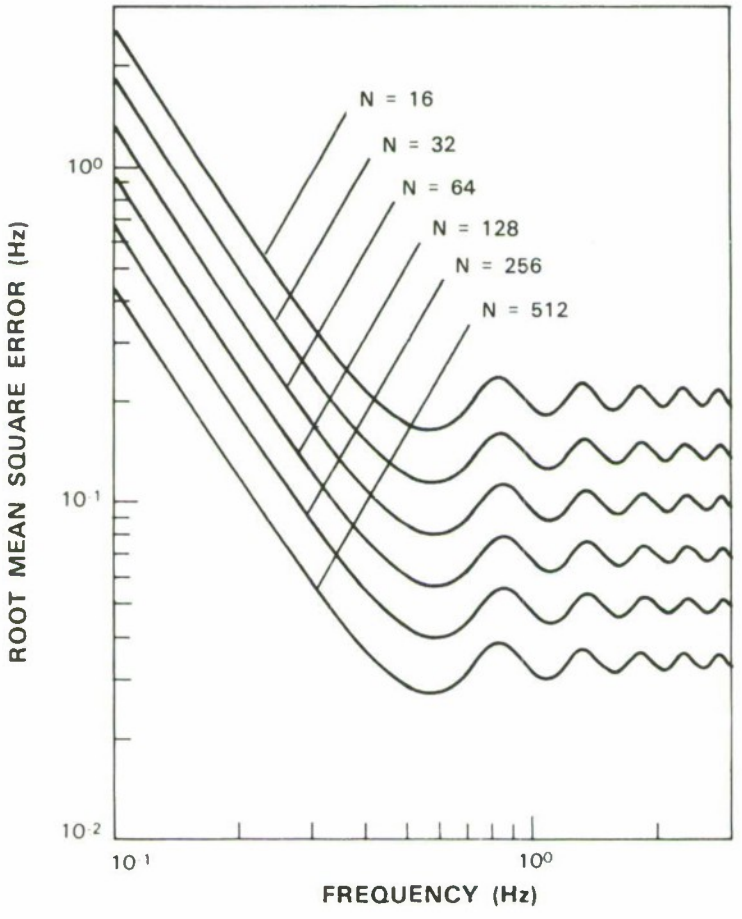

73645-3

Figure 3. Cramér-Rao bound for frequency estimation. $\phi = 0$, $\Delta N = 1$.

IV. DERIVATION OF THE ASYMPTOTIC CRAMÉR-RAO BOUND ($\phi = 0$)

The analytical problem is to simplify the summations which form the terms of the Fisher information matrix. It is of interest to examine the case in which trigonometric oscillatory terms in the Fisher information matrix, which depend on frequency, are summed [6]:

$$
\begin{aligned}
B_{11} &= N/2 \\
B_{22} &= (2\pi\Delta)^2 \left(\frac{N^3}{6} + \frac{N^2}{2} + \frac{N}{12}\right) \\
B_{33} &= N/2 \\
B_{12} &= B_{21} = 0 \\
B_{13} &= B_{31} = 0 \\
B_{23} &= B_{32} = (2\pi\Delta) \left(\frac{N^2}{4} + \frac{N}{2}\right)
\end{aligned}
\tag{9}
$$

It has been observed that the asymptotic levels of the Cramér-Rao bound $(B^{22})^{1/2}$, in the periodically decaying region between frequencies designated by the Nyquist criterion, can be calculated according to (9) as functions of N and Δ.

For Figures 2 and 3 this region of frequencies falls to the right of the first break point where $f > 1/2N\Delta$. This is equivalent to the condition that half the period $T/2$ is exceeded by the observation interval $N\Delta$. The Cramér-Rao bound can be approximated from (9) for frequencies to the right of the break points where the bound levels off, however, to only as far as $1/2N\Delta$ less than the first $f = 1/2\Delta$ Nyquist infinity. Subsequently, the Cramér-Rao bound can be obtained in this manner for respective frequencies in the higher order Nyquist periods.

Solving for $(B^{22})^{1/2}$, the asymptotic form for the Cramér-Rao bound for frequencies in the periodically decaying region is obtained:

$$
(B^{22})^{1/2} = \left(\frac{1}{2\pi\Delta}\right)\left(\frac{24}{N(N^2 - 10)}\right)^{1/2} \tag{10}
$$

Substituting for N and Δ, it is found that the values of this expression equal almost precisely the frequency independent asymptotic levels for the Cramér-Rao bounds which are shown partially in Figures 2 and 3. In the following table (Table 1) are values of $(B^{22})^{1/2}$ which were computed from (9) alongside those derived from the full Fisher information matrix (8).

Substitution of the sine and cosine series representations for small arguments into Equations (8) ($\phi = 0$) has also been achieved. This has determined that the asymptotic frequency dependence of the Cramér-Rao bound at low frequencies is proportional to $1/f^2$ for $\phi = 0$.

TABLE 1
Calculated Asymptotic Cramér-Rao Bound

N	Δ	$(B^{22})^{1/2}$	
		from (9)	from (10)
16	0.008	1.61	1.55
32	0.008	0.55	0.54
64	0.008	0.19	0.19
128	0.008	0.068	0.068
256	0.008	0.024	0.024
512	0.008	0.008	0.008
16	0.0625	0.206	0.199
32	0.0313	0.141	0.138
64	0.0156	0.099	0.098
128	0.0078	0.070	0.069
256	0.0039	0.049	0.049
512	0.002	0.034	0.034

V. NUMERICAL RESULTS FOR NON-ZERO PHASE

Figure 4 depicts the Cramér-Rao bound as a function of frequency when $\phi = 0$, $\pi/4$, $\pi/2$ and $3\pi/4$ for the case in which N = 64 and $\Delta = 0.008$. The bound was computed from the full Fisher information matrix (8). It can be discerned that the oscillations decay so that asympotically the curves all approach a single Cramér-Rao bound level equal to that for $\phi = 0$, N = 64, $\Delta = 0.008$ (Figure 2). The frequency dependence of the bound at low frequencies, for $\phi = \pi/2$, is determined to be 1/f. For frequencies less tha 0.2 Hz, the asymptotic behavior of the Cramér-Rao bounds for $\phi = 0$ and $\phi = \pi/2$ form an envelope about all of the phases shown in Figure 4.

Figure 5 departs from Figure 3 by only a small amount for f > 1. Figure 3 was obtained with $\phi = 0$. The former is created by taking the Cramér-Rao bound [computed from Equations (8)] with the phase which yields the highest Cramér-Rao bound out of 100 phases

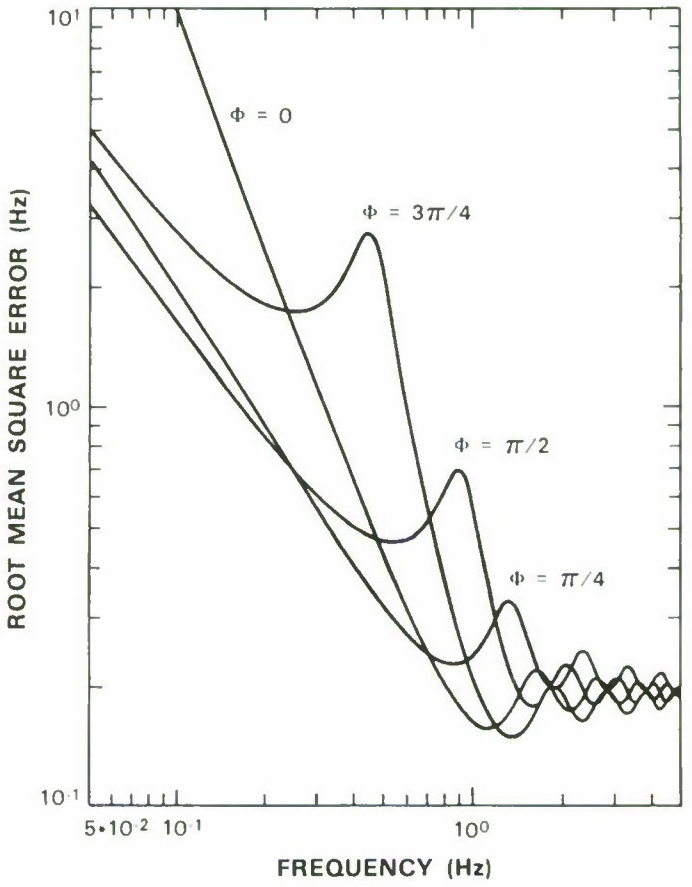

73645-4

Figure 4. Cramér-Rao bound for frequency estimation. N = 64, Δ = 0.008.

equally spaced between 0 and π. The behavior of the Cramér-Rao bound for worst case phase has already been shown in [2], however, this is for the case of a constant sampling interval Δ and large frequency.

$N\Delta$ is constrained to be equal to 1 for both Figures 3 and 5. The break point between the monotonic and periodic segments in the family of curves in Figure 5 occurs at approximately $f = 1/N\Delta$, while for Figure 3 is at approximately $1/2N\Delta$. The lower break point for the case of $\phi = 0$ is equal to the first null in sin Nw/sin w, where $w = \pi/N$, and $w = 2\pi f\Delta$, which is exactly $f = 1/2N\Delta$.

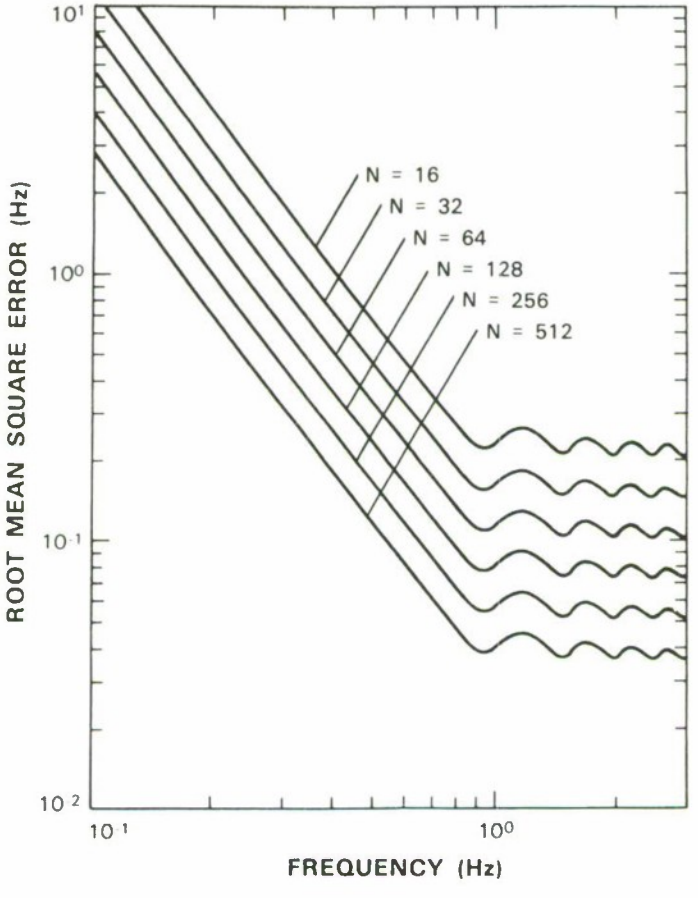

73645-5

Figure 5. Cramér-Rao bound for frequency estimation. Worst case ϕ. $\Delta N = 1$.

VI. NORMALIZATION OF THE CRAMÉR-RAO BOUND: TRADE-OFFS INVOLVING NΔ AND SNR

One conclusion which can be drawn from Figures 2 and 3 in the previous section is that the width of the main lobe of the Cramér-Rao bound curves is the parameter $1/2N\Delta$. This can be identified with the resolution of the estimation process. The greater the observation interval $N\Delta$, the smaller will be the resolution $\delta f = 1/2N\Delta$. This trend can be likened to that of a square wave and its Fourier transform. The wider the square wave is, the smaller the width to the first null of its Fourier transform will be.

In Figure 6, the Cramér-Rao bound σ_f normalized by the resolution $\delta f = 1/2N\Delta$ is plotted against the frequency normalized by δf. This is achieved for N = 16, 32, 64, 128, 256, and 512, for $\Delta = 0.008$ in each case. These are the same parameters as were used for the unnormalized case in Figure 2. The curves of the family which results all break at the same $f/\delta f$ and are separated by a constant multiple for all $f/\delta f$.

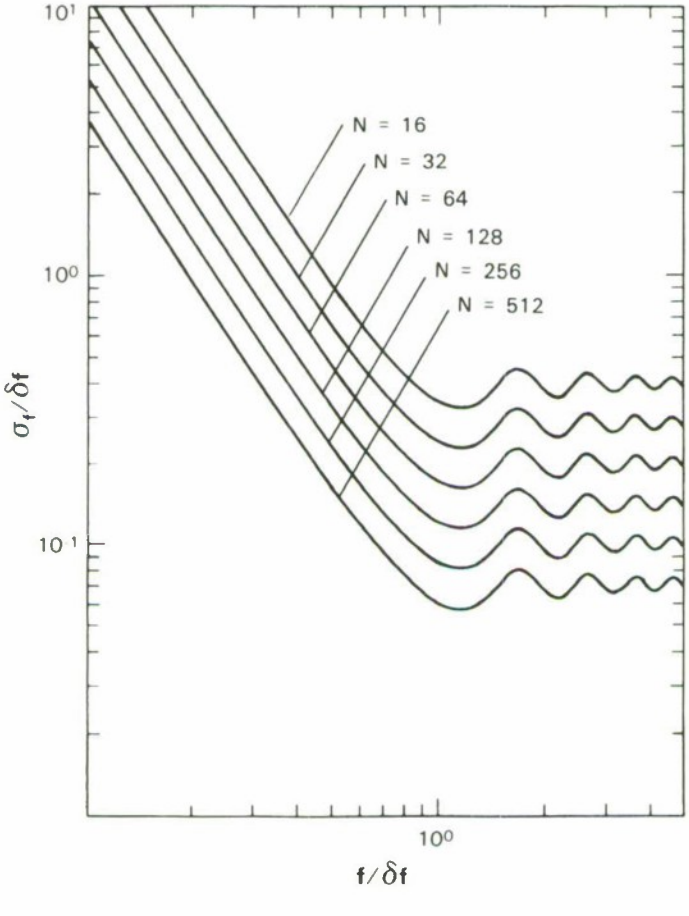

73645-6

Figure 6. Normalized Cramér-Rao bound for frequency estimation. $\phi = 0$

It was shown in Equation (10) of Section IV that the asymptotic Cramér-Rao bound is on the order of $1/N^{3/2}\Delta$. Thus the normalized Cramér-Rao bound $\sigma_f/\delta f$ is on the order of $1/\sqrt{N}$. Another piece of information we can extract from scaling the Cramér-Rao bound is that the family of curves in Figure 6 can be collapsed to one of $\sqrt{N}\ \sigma_f/\delta f$ versus $f/\delta f$. This is shown in Figure 7 where for numerical convenience another scaling factor $\sqrt{1/64}$ has been included. The family of curves is thus represented by the single relationship of $\sqrt{N/64}\ \sigma_f/\delta f$ versus $f/\delta f$.

From Figure 7 it can be observed that, in the low frequency region where $f < 1/2N\Delta$, the slope of the curve is approximately –2, for $\phi = 0$.

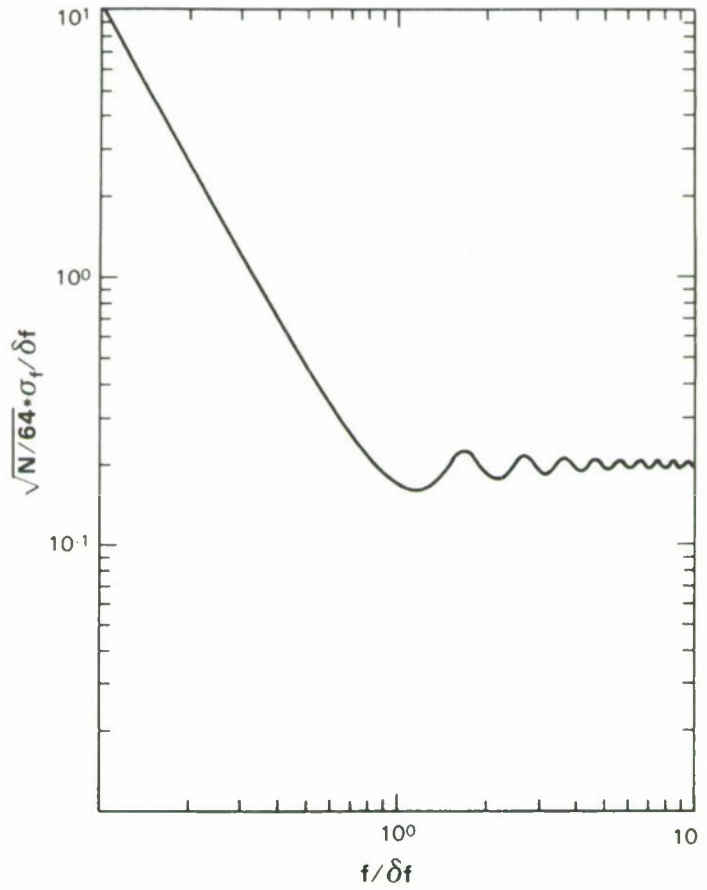

73645-7

Figure 7. Fully normalized Cramér-Rao bound.

$$\text{Thus } \sqrt{N/64}\ \frac{\sigma_f}{\delta f} \approx \frac{C}{\left(\frac{f}{\delta f}\right)^2} \text{ or } \sigma_f \approx \frac{C}{N^{7/2}\Delta^3 f^2} \tag{11}$$

$$\text{where } \delta f = \frac{1}{2N\Delta} \text{ and } C \approx 0.1$$

This relation represents the dependence of the Cramér-Rao bound on frequency, for low frequencies mapped onto the limb of the curve which lies to the left of the break point.

The following examples are designed to exemplify the trade-offs of $N\Delta$ and SNR which can be determined using Figure 7.

Example 1: Given $f = 2$ Hz, $\delta f = 1$ Hz, and SNR = 1, what are N and Δ such that the Cramér-Rao bound σ_f equals 0.1?

For $f/\delta f = 2$, it is shown in Figure 8 that $\sqrt{N/64}\ \sigma_f/\delta f$ equals approximately 0.2. Since $\sigma_f/\delta f = 0.1$, N can be solved for and is found to be 256. It is also known that $\delta f = 1/2N\Delta = 1$ Hz, so with $N = 256$, Δ need be no larger than 0.002.

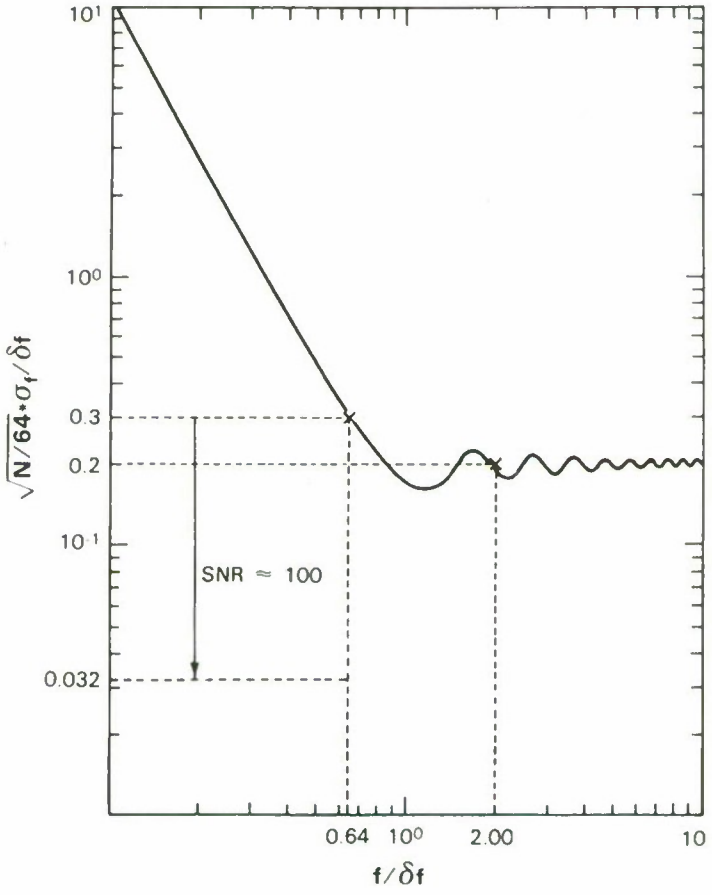

73645-8

Figure 8. Fully normalized Cramér-Rao bound (example 1, 2).

For the second example, SNR is for the first time a variable parameter and is no longer set equal to 1. It can be discerned from Equation set (8) that $(B^{22})^{1/2}$, the Cramér-Rao bound, will be proportional to $1/A/\sigma_R$ or $1/\sqrt{SNR}$.

Example 2: Using Figure 7, the problem here is to determine what SNR ratio is necessary so that $\sigma_f = 0.2$ Hz when $f = 2$ Hz, $N = 16$, and $\Delta = 0.01$.

It is known that $\delta f = 1/2N\Delta = 1/0.32$ Hz so that $f/\delta f = 0.64$. The design point for which $\sqrt{SNR}$ will be determined is, for $N = 16$, at $\sqrt{16/64}\ \sigma_f/\delta f$. When $\sigma_f = 0.2$ Hz and $\delta f = 1/0.32$ Hz, this point falls at 0.032 on the vertical axis of Figure 8. However, the actual point on the axis to which $f/\delta f = 0.64$ corresponds is approximately 0.3. Therefore a $\sqrt{SNR}$ ratio of ≈ 10 is required to reduce the normalized and scaled value of the Cramér-Rao bound from ≈ 0.3 to 0.032.

VII. SUMMARY AND CONCLUSIONS

The influences of number of samples, sampling frequency, phase, and signal-to-noise ratio on the Cramér-Rao bound for frequency estimation of sine waves in Gaussian white noise have been studied. A closed form expression for the asymptotic Cramér-Rao bound has been derived which exhibits a $1/N^{3/2}\Delta$ dependence. The Cramér-Rao bound normalized by the resolution and scaled by $\sqrt{N}$, where N is the number of samples, reduces the family of curves parameterized by N and Δ to a single operating curve. Examples of trade-offs involving $N\Delta$ and SNR ratio are determined by this composite relationship among the parameters.

As long as the measurement interval $N\Delta$ is at least a half cycle of the sine wave, the Cramér-Rao bound is close to being independent of frequency; however, in the instance of worst case phase the measurement interval must cover an entire cycle. In the low frequency region where $N\Delta$ is less than half a cycle, the bound on σ_f varies as $1/f^2$ for phase $\phi = 0$, and $1/f$ for phase $\phi = \pi/2$. For example, if the frequency is 0.1 Hz, the value of σ_f will be at most 25 times larger than for a frequency of 0.5 Hz, with the same parameters N, Δ. If the signal-to-noise is sufficiently high, it is still possible to obtain accurate frequency estimates even in this low frequency region.

ACKNOWLEDGMENTS

I wish to thank Dr. Keh-Ping Dunn, Dr. Daniel O'Connor, and Dr. Stephen Weiner for their help and suggestions in preparing this paper. The programming assistance of Mr. Paul Warren is gratefully acknowledged. I also wish to express my appreciation to Miss Nancy Asadoorian and Miss Laura Parr for their typing expertise.

REFERENCES

1. D.C. Rife and R.R. Boorstyn, "Single-tone Parameter Estimation from Discrete-Time Observations," IEEE Trans. Inf. Theory **IT-20** (September 1974).
2. D.C. Rife and R.R. Boorstyn, "Multiple Tone Parameter Estimation from Discrete-Time Observations," Bell Syst. Tech. J. **55** (November 1976).
3. M.J. Tsai, "The ML Method for Frequency Estimation of Real Sinusoids in Noise," Technical Report 689, Lincoln Laboratory, MIT (27 July 1984), DTIC AD-A146053.
4. H.L. Van Trees, *Detection, Estimation, and Modulation Theory* Part 1 (Wiley, New York, 1968).
5. D. Slepian, "Estimation of Signal Parameters in the Presence of Noise," IRE Trans. Inf. Theory **PGIT-3** (March 1954).
6. L.B.W. Jolley, *Summation of Series* (Dover, New York, 1961).

UNCLASSIFIED

SECURITY CLASSIFICATION OF THIS PAGE *(When Data Entered)*

REPORT DOCUMENTATION PAGE		READ INSTRUCTIONS BEFORE COMPLETING FORM
1. REPORT NUMBER ESD-TR-85-323	2. GOVT ACCESSION NO.	3. RECIPIENT'S CATALOG NUMBER
4. TITLE *(and Subtitle)* Cramér-Rao Bound Analysis for Frequency Estimation of Sinusoids in Noise		5. TYPE OF REPORT & PERIOD COVERED Technical Report 6. PERFORMING ORG. REPORT NUMBER Technical Report 727
7. AUTHOR(s) Joy M. Skon		8. CONTRACT OR GRANT NUMBER(s) F19628-85-C-0002
9. PERFORMING ORGANIZATION NAME AND ADDRESS Lincoln Laboratory, MIT P.O. Box 73 Lexington, MA 02173-0073		10. PROGRAM ELEMENT, PROJECT, TASK AREA & WORK UNIT NUMBERS Program Element Nos. 63220C and 63304A
11. CONTROLLING OFFICE NAME AND ADDRESS U.S. Army Strategic Defense Command — Huntsville Sensors Directorate P.O. Box 1500 Huntsville, AL 35807-3801		12. REPORT DATE 24 March 1986 13. NUMBER OF PAGES 22
14. MONITORING AGENCY NAME & ADDRESS *(if different from Controlling Office)* Electronic Systems Division Hanscom AFB, MA 01731		15. SECURITY CLASS. *(of this Report)* Unclassified 15a. DECLASSIFICATION DOWNGRADING SCHEDULE

16. DISTRIBUTION STATEMENT *(of this Report)*

Approved for public release; distribution unlimited.

17. DISTRIBUTION STATEMENT *(of the abstract entered in Block 20, if different from Report)*

18. SUPPLEMENTARY NOTES

None

19. KEY WORDS *(Continue on reverse side if necessary and identify by block number)*

Cramér-Rao bound	signal-to-noise ratio
frequency estimation	resolution
sampling frequency	sinusoids

20. ABSTRACT *(Continue on reverse side if necessary and identify by block number)*

The Cramér-Rao inequality is used to determine a lower bound on the variance with which a sinusoidal frequency can he estimated in the presence of Gaussian white noise. A parametric study has elucidated the influence of number of samples (N), sampling frequency ($1/\Delta$), phase (ϕ), and signal-to-noise ratio (SNR) on the Cramér-Rao bound. A closed form expression for the asymptotic level to which the Cramér-Rao bound decays is characterized and, for low frequencies, the bound is determined analytically and graphically. The form of the Cramér-Rao bound is linked to resolution in the sampling prohlem. Identification of trade-offs characterizing the sensitivity of the bound and parameters associated with it are discussed.

DD FORM 1 Jan 73 1473 EDITION OF 1 NOV 65 IS OBSOLETE

UNCLASSIFIED

SECURITY CLASSIFICATION OF THIS PAGE *(When Data Entered)*